# Multistep Solid-State Organic Synthesis of Carbamate-Linked Covalent Organic Frameworks

Steven J. Lyle,[†] Thomas M. Osborn Popp,[†,‡] Peter J. Waller,[†] Xiaokun Pei,[†] Jeffrey A. Reimer,[‡] and Omar M. Yaghi*[,†,§]

[†]Department of Chemistry, University of California—Berkeley, Materials Sciences Division, Lawrence Berkeley National Laboratory, Kavli Energy NanoSciences Institute at Berkeley and Berkeley Global Science Institute, Berkeley, California 94720, United States

[‡]Department of Chemical and Biomolecular Engineering, Environmental Energy Technologies Division, Lawrence Berkeley National Laboratory, University of California—Berkeley, Berkeley, California 94720, United States

[§]King Abdulaziz City for Science and Technology, Riyadh 11442, Saudi Arabia

**ABSTRACT:** Herein, we demonstrate the first example of a multistep solid-state organic synthesis, in which a new imine-linked two-dimensional covalent organic framework (COF-170, **1**) was transformed through three consecutive post-synthetic modifications into porous, crystalline cyclic carbamate and thiocarbamate-linked frameworks. These linkages are previously unreported and inaccessible through *de novo* synthesis. While not altering the overall connectivity of the framework, these chemical transformations induce significant conformational and structural changes at each step, highlighting the key importance of noncovalent interactions and conformational flexibility to COF crystallinity and porosity. These transformations were assessed using $^{15}$N multiCP-MAS NMR spectroscopy, providing the first quantitation of yields in COF postsynthetic modification reactions, as well as of amine defect sites in imine-linked COFs. This multistep COF linkage postsynthetic modification represents a significant step toward bringing the precision of organic solution-phase synthesis to extended solid-state compounds.

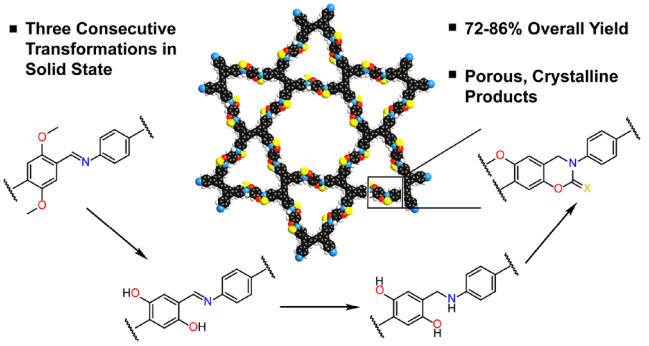


## INTRODUCTION

Covalent organic frameworks (COFs) are a class of designed, porous, crystalline materials built from the covalent linkage of geometrically predefined building units into two- and three-dimensional extended networks.[1,2] The ability to control the relative positioning of chemical functionalities in covalently linked solids represents an extension of organic chemistry into the solid state.[3,4] This extension includes not only the ability to crystallize these ordered networks from molecular building blocks but also the ability to treat the extended solids as molecules. It has been demonstrated in numerous cases that chemical transformations can take place on COFs much as they do in solution due to the ability of reactants and byproducts to diffuse through the pores of a COF.[5−7] Notably, postsynthetic modifications can be performed on COF linkages without alteration of topology.[8−12] Linkage transformations, in particular, distinguish themselves from reactions performed on molecules appended to solid supports, such as solid-phase peptide synthesis, because the stability, reactivity, and structure of a COF is largely defined by its linkages.[13,14]

Postsynthetic modification allows access to new linkage functionalities without the need to develop reaction conditions capable of directly generating an ordered network reticulated by those linkages. This has been demonstrated for a number of imine-linked COFs, the linkages of which were converted to secondary amides, secondary amines, thiazoles, oxazoles, and quinolines.[8−12] However, amide- and oxazole-linked COFs have been formed directly from molecular building units,[15,16] and in principle, each of these linkages could be made directly, by employing a one-pot strategy whereby COFs are formed from a reversible imine condensation followed by a less reversible or irreversible second step *in situ*.[17−20]

In organic synthesis, we are not limited to compounds accessible in a single synthetic step. The translation of multistep organic synthesis to the solid state, however, requires extending not only the chemistry but also the rigor of characterization found in small-molecule synthesis to solids. Herein, we describe the first extension of both these features of organic chemistry to covalent solids, achieved by the multistep postsynthetic modification of a COF to generate porous, crystalline cyclic carbamate and thiocarbamate-linked frameworks accessible only through multistep synthesis. Each reaction in this synthesis involves transformation of the

**Scheme 1. Synthesis of Cyclic Carbamate and Thiocarbamate-Linked COFs by a Three-Step Solid-State Synthesis**

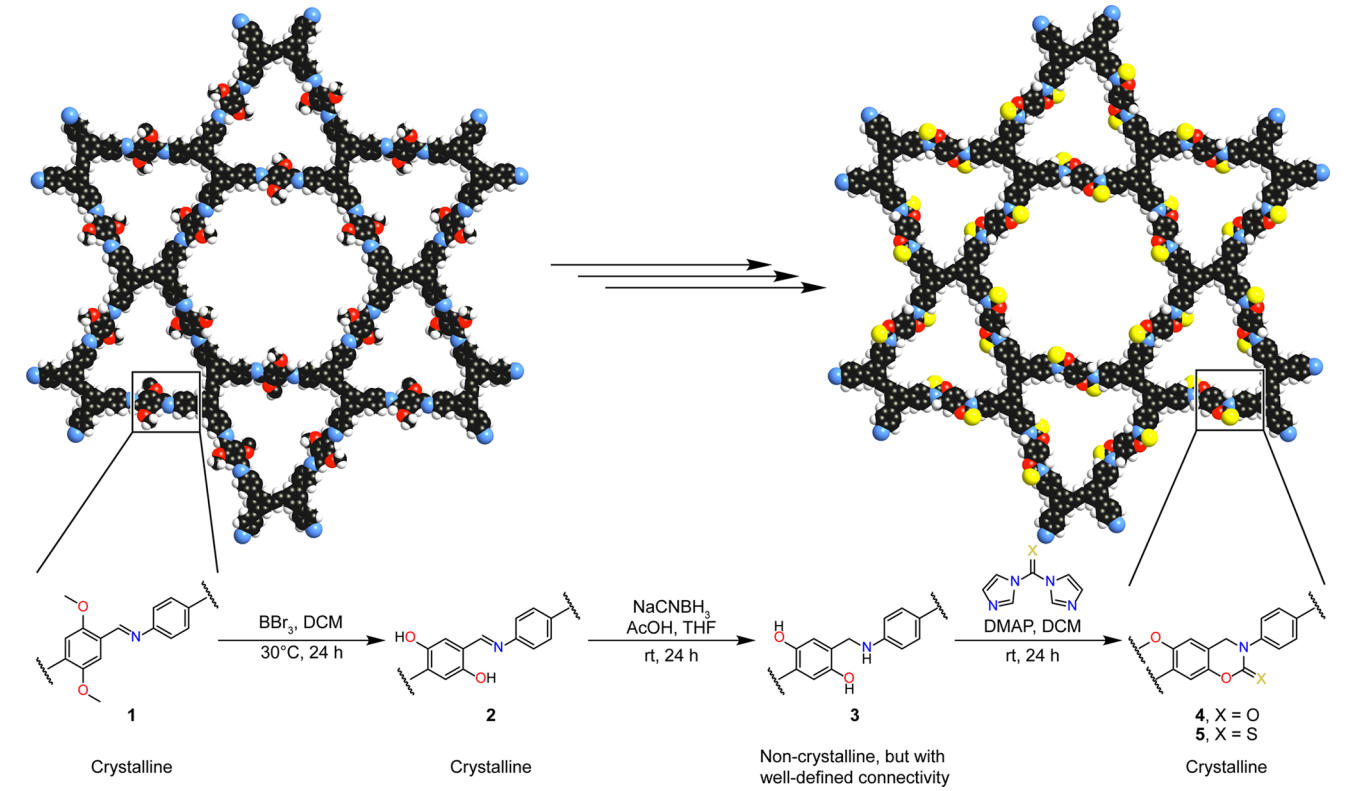


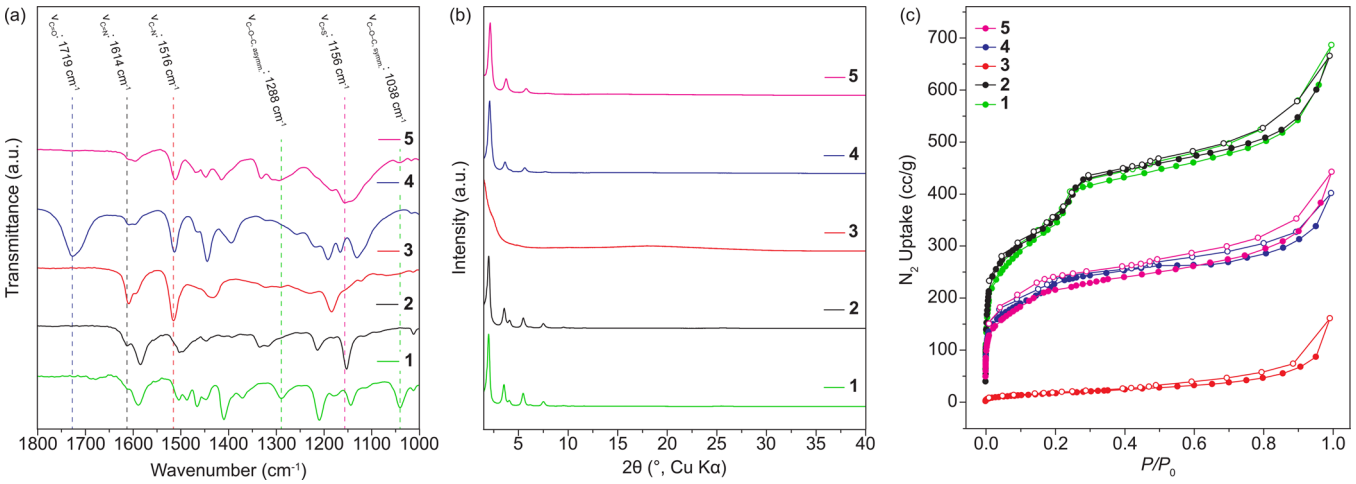


**Figure 1.** (a) FT-IR spectra of COFs **1**–**5**, labeled with diagnostic stretching frequencies reported for each linkage. (b) PXRD patterns of COFs **1**–**5**, demonstrating the retention of crystallinity through all but amine-linked **3**. (c) $N_2$ adsorption isotherms performed at 77 K for COFs **1**–**5**, displaying permanent porosity for all but amine linked **3**. Solid and open circles designate adsorption and desorption points, respectively. Uptake is defined as $cm^3$ of $N_2$ at 1 atm and 0 °C per gram of sample.

material's linkage and as such occurs with concomitant structural changes, but preservation of the underlying topology. Furthermore, each compound was analyzed by $^{15}N$ multiple cross-polarization magic angle spinning nuclear magnetic resonance spectroscopy (multiCP-MAS NMR), allowing for the first quantitative evaluation of chemical transformations in COFs. This work sets a new standard for the execution and evaluation of multistep chemical transformations of solids and in doing so lays the groundwork for further exploration of solid-state organic synthesis.

## RESULTS AND DISCUSSION

A new **kgm** topology COF, COF-170 (**1**), was synthesized solvothermally from the condensation of (*E*)-3,3′,5,5′-tetrakis-(4-aminophenyl)stilbene (TAPS) and 3,5-dimethoxyterephthalaldehyde (DMTP) in a 5:5:1 mixture of *o*-dichlorobenzene, 1-butanol, and 6 M AcOH at 120 °C for 3 days. COF-170 served as the starting material for the synthesis of isostructural cyclic carbamate- and thiocarbamate-linked COFs (Scheme 1). This synthesis began first with demethylation of **1**'s methoxy groups, followed by reduction of the imine linkage with sodium cyanoborohydride and acetic acid in THF.[21] This

amine-linked COF (**3**) was then treated with 1,1′-carbonyldiimidazole (CDI) or 1,1′-thiocarbonyldiimidazole (TCDI) and *N*,*N*-dimethylaminopyridine (DMAP) in dichloromethane to yield cyclic carbamate- (**4**) and thiocarbamate- (**5**) linked COFs, respectively.[22] Between each of these steps, and prior to characterization, the intermediate compounds were subjected to thorough solvent exchange and activation to prepare the material for the subsequent transformation. In order to provide rigorous data consistency, all characterization, including $^{15}$N multiCP-MAS NMR spectroscopy, was performed on the same 33% $^{15}$N-labeled samples. All relevant synthetic procedures can be found in sections 2−4 of the Supporting Information.

The progress of these transformations was initially monitored by FT-IR spectroscopy (Figure 1a). Demethylation of **1**'s methoxy groups was observed through the disappearance of its ether C−O−C symmetric and asymmetric stretches at 1038 and 1288 cm$^{-1}$, respectively.[23] Upon reduction of the imine linkages of **2**, we observed the disappearance of its imine C═N stretch at 1614 cm$^{-1}$ and the emergence of an amine C−N stretch at 1516 cm$^{-1}$.[10] After cyclization to carbamates and thiocarbamates, characteristic C═O and C═S stretches were observed at 1719 and 1156 cm$^{-1}$, respectively, and corroborated by comparison to molecular models (see SI, section S5).[24]

Although diagnostic, FT-IR spectroscopy alone does not constitute evidence of reaction completeness and in this context cannot provide quantitative information on the composition of the analyzed COFs. $^{15}$N solid-state NMR spectroscopy provides an alternative means to clearly track the conversion between linkages across the multiple steps of this synthetic process. While commonly employed in the characterization of COF linkage transformations, traditional CP-MAS NMR does not provide quantitative integrations of resonances due to variable polarization rates between $^{1}$H and the target nucleus across different chemical functionalities. Quantitative solid-state NMR spectra may be achieved by direct observation of $^{15}$N; however, long $T_1$ relaxation times combined with the low sensitivity of the nucleus can make these measurements impractical. MultiCP-MAS NMR spectroscopy provides a means to measure quantitative solid-state NMR spectra in solids with reasonable measurement times.[25,26] To date, the multiCP method has only been applied to the measurement of $^{13}$C NMR spectra. In applying this method to $^{15}$N, we found it necessary to enrich the sample due to its low natural abundance. However, full enrichment was not necessary to obtain routine spectra.

$^{15}$N multiCP-MAS NMR of 33% $^{15}$N-labeled substrates yielded quantitative insight into the postsynthetic modification process (Figure 2). In the spectrum of each COF, the primary resonance observed corresponds to the major product of the preceding reaction step. As the resonances for each chemical site showed some degree of inhomogeneous broadening due to structural disorder, resonances corresponding to different sites were fit to Gaussian lineshapes, and their relative areas were compared (see SI, section S6). Using this method, the composition of each COF along the synthetic pathway was analyzed (Table 1). In imine-linked COFs **1** and **2**, residual primary amine sites were found to make up 6 and 8% of total $^{15}$N sites, respectively. The chemical shifts of the imine sites within these two materials are distinct enough to enable monitoring of the demethylation step, which occurred in 91% yield. The reduction of imine species in **2** to make **3** was found to be complete within the detection limit of the NMR experiment. In contrast to the imine resonances, the chemical shifts of the methoxy-adjacent, hydroxy-adjacent, and primary amine linkages cannot be clearly resolved. Nonetheless, the relative composition of secondary amine linkages can be

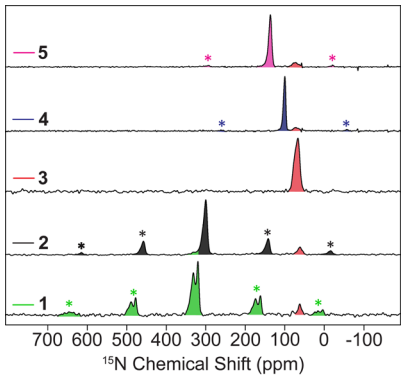


**Figure 2.** $^{15}$N multiCP-MAS NMR spectra of 33% $^{15}$N-labled COFs **1**−**5**, colored to highlight the composition of each sample. Spinning side bands are indicated by asterisks.

**Table 1. Linkage Composition of COFs 1−5, Determined from Peak Fitting of $^{15}$N MultiCP-MAS NMR Spectra**[a]

| Linkage Species | Composition (%) | | | | |
|---|---|---|---|---|---|
| | **1** | **2** | **3** | **4** (X=O) | **5** (X=S) |
| 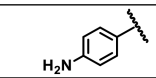 | 6 | 8 | 8 | 0-8 | 0-8 |
| 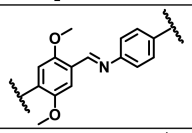 | 94 | 8 | 0 | 0 | 0 |
| 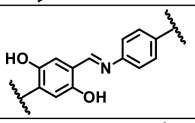 | — | 84 | 0 | 0 | 0 |
| 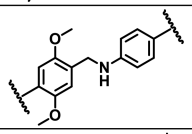 | — | — | 8 | 0-8 | 0-8 |
| 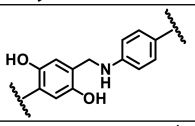 | — | — | 84 | 0-14 | 0-14 |
| 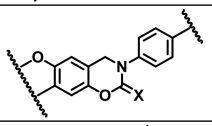 | — | — | — | 72-86 | 72-86 |
| 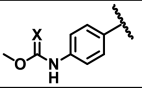 | — | — | — | 0-8 | 0-8 |
| 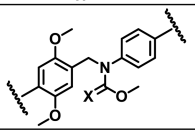 | — | — | — | 0-8 | 0-8 |

[a]Composition ranges given for **4** and **5** reflect the fact that primary amines and secondary amines with adjacent methoxy groups present in **3** may be forming *O*-methyl carbamate and thiocarbamate species which contribute to the observed carbamate and thiocarbamate resonances.

inferred under the assumption that the amount of primary amine remains unchanged after the reduction. Treatment of **3** with CDI and DMAP affords a material **4** in which 86% of $^{15}$N sites are carbamates, and the remainder are a mixture of amine sites. Thiocarbamate-linked **5** shows a similar conversion of 86% thiocarbamate with 14% mixed amines remaining. The carbamate and thiocarbamate resonances in **4** and **5** are likely a mixture of species, as only the secondary amine with an adjacent hydroxyl group can form cyclic carbamates or thiocarbamates. The primary amines and the secondary amines with adjacent methoxy groups are capable of generating *O*-methyl carbamates and *O*-methyl thiocarbamates from the addition of those amines to CDI or TCDI followed by quenching with methanol during the solvent exchange process.[27,28] For this reason, the yields of cyclic carbamate and cyclic thiocarbamate are reported as a range that considers the possibility that the *O*-methyl species may be contributing to the observed resonance.

Having determined the composition of these COFs, we sought to understand their structures in more detail and how they may have changed during the synthetic pathway. COFs **1**−**5** were evaluated by powder X-ray diffraction (PXRD) and $N_2$ adsorption isotherm experiments (Figure 1b,c). Pawley fitting of imine-linked COFs **1** and **2** shows good agreement with simulated structures, confirming that their connectivity and **kgm** topology are preserved during the demethylation step (see SI, section S7). Additionally, both **1** and **2** are porous, with Brunauer−Emmett−Teller (BET) areas of 1229 and 1233 $m^2/g$, respectively. While these experiments confirm the topology and porosity of these materials, they do not provide a complete picture of the structures of **1** and **2**. Due to the broad diffraction peaks common to most COF materials, the diffraction data cannot provide enough information to determine the orientation of the methoxy- or hydroxy-substituted phenyl rings relative to the imine bond. The orientation of this ring relative to the linkage is critical to the formation of cyclic carbamates, as the cyclization cannot proceed unless the amine and hydroxyl group are positioned along the same side in close proximity. To gain insight into the possible orientations of this site in each imine-linked COF structure, molecular models of **1** and **2** were synthesized, and their structures were determined by single-crystal X-ray diffraction (see SI, section S11). For the model of **1**, it was found that the methoxy groups position themselves opposite the imine bond to minimize steric interactions, while the hydroxy groups in **2**'s model compound position themselves on the same side as the imine to form intramolecular hydrogen bonds. The differences in energy between the two possible phenyl orientations were explored for each model compound by gas-phase DFT simulations (see SI, section S12). For the hydroxy- and methoxy-substituted model compounds, the orientations observed in the crystal structures were found to be preferred by 62.5 and 39.6 kJ/mol, respectively. $^{15}$N NMR chemical shifts for each orientation of the model compounds were calculated (see SI, section S12) and suggest that these species should be distinguishable by our $^{15}$N NMR experiments. Comparing these predictions to experiment, not only are the methoxy-adjacent and hydroxy-adjacent imine sites distinguishable between the $^{15}$N spectra of **1** and **2** but also **1** contains two independent imine resonances. Based on the insights gained from the crystal structures and DFT calculations of the model compounds, we believe that both orientations of the methoxy-substituted phenyl ring are present in **1**, and only the orientation which yields intramolecular hydrogen bonding is present in **2**. This suggests that upon demethylation the COF undergoes a structural rearrangement to adopt its most stable conformation (Scheme 2).

**Scheme 2. Reorientation of Hydroxyl Groups in the Solid State after Demethylation**

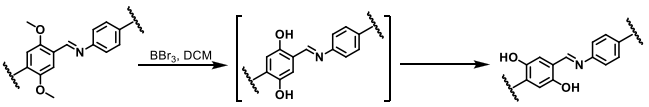


In contrast to **1** and **2**, amine-linked **3** is noncrystalline and less porous, with a BET area of only 61 $m^2/g$. Based on these results, it would appear the COF had irreversibly degraded after the reduction; however, carrying the synthesis through to generate **4** or **5** yields materials which are both crystalline and porous. Pawley fitting of the diffraction data for **4** and **5** shows good agreement with their respective model structures, confirming that they possess both the connectivity and eclipsed stacking arrangement of their imine progenitor **1** (see SI, section S7). Additionally, the BET areas of **4** and **5** were found to be 780 and 791 $m^2/g$, retaining 64 and 63% of the BET area of **1**, respectively. This retention of surface area occurs despite the COF being subjected to three consecutive postsynthetic modifications, one of which resulted in a noncrystalline framework. From these experiments, we can infer that **3** possesses the same topology as **1**, **2**, **4**, and **5**, despite a lack of crystallinity. The loss of crystallinity and porosity upon reduction of **2** and its subsequent reemergence in **4** and **5** can be attributed to the conformational flexibility of the secondary amine linkages of **3**. In contrast, imines, cyclic carbamates, and cyclic thiocarbamates are significantly less conformationally flexible and adopt comparatively planar conformations as observed in molecular model crystal structures (see SI, section S11).

This same pattern of crystallinity loss and recovery can be observed from the reduction of the imine linkages of **1** to amines, followed by reoxidation back to imines with 2,3-dichloro-5,6-dicyano-1,4-benzoquinone (DDQ).[29] Both the starting and ending imine-linked materials are crystalline, while the intermediate amine is noncrystalline. Loss and recovery of crystallinity upon reduction and reoxidation of the imine linkage is even observed for ILCOF-1, despite the presence of strongly stacking pyrene units and a smaller pore size than **1** (see SI, section S13).[30] Dynamics of this type have previously been observed in molecular crystals, as well the woven COF-505, for which crystallinity can be lost and recovered by the removal and reintroduction of $Cu^+$ templates within the structure.[31,32]

In an effort to evaluate the necessity of performing the demethylation of **1** in the solid state, we examined the synthesis of **4** and **5** starting from *de novo* synthesized **2** (**2′**), which can be formed directly from the condensation of TAPS and 3,5-dihydroxyterephthalaldehyde (see SI, section S3). This would shift the demethylation, which we know to be incomplete in the solid state under our conditions, to the solution state. Even after extensive screening of crystallization conditions, **2′** possesses poorer crystallinity and significantly lower surface area than **2** (see SI, section S10). The quality of this COF has a significant impact on subsequent postsynthetic modifications (see SI, section S6). Despite being performed

under identical conditions, reduction under this route proceeds at only 80% yield. Subsequent treatment with CDI or TCDI and DMAP yields **4′** and **5′**, in which only 62 and 68% of $^{15}N$ sites are carbamates and thiocarbamates, respectively. Furthermore, the BET areas of **4′** and **5′** are only 217 and 332 $m^2/g$ respectively. The differences between these two synthetic routes illustrate the importance of the quality of COF starting material in postsynthetic modifications. In this case, one additional synthetic step in the solid state provides access to significantly higher yields and higher quality products due to our ability to access a more crystalline and porous COF starting material.

## CONCLUSIONS

In conclusion, an imine-linked COF was transformed through three consecutive synthetic steps to isostructural cyclic carbamate- and thiocarbamate-linked COFs. These new linkages are the first for which one-pot small-molecule equivalent reactions do not exist, necessitating the need for multistep synthesis in the solid state. Each substrate in this synthesis was analyzed by $^{15}N$ multiCP-MAS NMR spectroscopy, for the first time allowing quantitative compositional analysis of each compound along the synthetic route. Furthermore, each solid-state chemical transformation performed in this work was accompanied by a structural or conformational transformation, highlighting the critical importance of linkages in COF structure and properties. This work constitutes an extension of organic synthesis—both multistep transformations and the analytical rigor necessary to characterize them—from the solution to the solid state.

## AUTHOR INFORMATION


### Corresponding Author

*yaghi@berkeley.edu

### ORCID

Steven J. Lyle: 0000-0003-2341-3177
Peter J. Waller: 0000-0002-4013-8827
Jeffrey A. Reimer: 0000-0002-4191-3725
Omar M. Yaghi: 0000-0002-5611-3325


### Notes

The authors declare no competing financial interest.

## ACKNOWLEDGMENTS


Synthesis in this work was supported by King Abdulaziz City for Science and Technology (Center of Excellence for Nanomaterials and Clean Energy Applications) and the characterization of compounds by the Center for Gas Separations Relevant to Clean Energy Technologies, an Energy Frontier Research Center funded by the U.S. Department of Energy, Office of Science, Basic Energy Sciences under Award DE-SC0001015. T.O.P. acknowledges funding from the NSF Graduate Research Fellowship Program and the Chevron-UC Berkeley Graduate Fellowship Program. We also acknowledge use of the computational resources in the Molecular Graphics and Computational Facility at UC Berkeley, which is supported under NIH S10OD023532. Crystal structures of model compounds **11** an **12** in the Supporting Information were obtained by Nicholas Settineri and were supported by the NIH Shared Instrumentation Grant S10 RR027172.


## REFERENCES


(1) Yaghi, O. M.; Kalmutzki, M. J.; Diercks, C. S. *Introduction to Reticular Chemistry: Metal-Organic Frameworks and Covalent Organic Frameworks*; Wiley-VCH Verlag GmbH & Co. KGaA: Weinheim, Germany, 2019; p 509.

(2) Waller, P. J.; Gándara, F.; Yaghi, O. M. Chemistry of Covalent Organic Frameworks. *Acc. Chem. Res.* **2015**, *48*, 3053−3063.

(3) Diercks, C. S.; Yaghi, O. M. The atom, the molecule, and the covalent organic framework. *Science* **2017**, *355*, 293−302.

(4) Lyle, S. J.; Waller, P. J.; Yaghi, O. M. Covalent Organic Frameworks: Organic Chemistry Extended into Two and Three Dimensions. *Trends in Chemistry* **2019**, *1* (2), 172−184.

(5) Nagai, A.; Guo, Z.; Jin, S.; Feng, X.; Jin, S.; Chen, X.; Ding, X.; Jiang, D. Pore surface engineering in covalent organic frameworks. *Nat. Commun.* **2011**, *2*, 536.

(6) Sun, Q.; Aguila, B.; Perman, J.; Earl, L. D.; Abney, C. W.; Cheng, Y.; Wei, H.; Nguyen, N.; Wojtas, L.; Ma, S. Postsynthetically Modified Covalent Organic Frameworks for Efficient and Effective Mercury Removal. *J. Am. Chem. Soc.* **2017**, *139* (7), 2786−2793.

(7) Lohse, M. S.; Stassin, T.; Naudin, G.; Wuttke, S.; Ameloot, R.; De Vos, D.; Medina, D. D.; Bein, T. Sequential Pore Wall Modification in a Covalent Organic Framework for Application in Lactic Acid Adsorption. *Chem. Mater.* **2016**, *28* (2), 626−631.

(8) Waller, P. J.; Lyle, S. J.; Osborn Popp, T.; Diercks, C. S.; Reimer, J. A.; Yaghi, O. M. Chemical Conversion of Linkages in Covalent Organic Frameworks. *J. Am. Chem. Soc.* **2016**, *138*, 15519−15522.

(9) Haase, F.; Troschke, E.; Savasci, G.; Banerjee, T.; Duppel, V.; Dörfler, S.; Grundei, M. M. J.; Ochsenfeld, C.; Kaskel, S.; Lotsch, B. V. Topochemical conversion of an imine- into a thiazole-linked covalent organic framework enabling real structure analysis. *Nat. Commun.* **2018**, *9*, 2600.

(10) Liu, H.; Chu, J.; Yin, Z.; Cai, X.; Zhuang, L.; Deng, H. Covalent Organic Frameworks Linked by Amine Bonding for Concerted Electrochemical Reduction of $CO_2$. *Chem.* **2018**, *4*, 1696−1709.

(11) Li, X.; Zhang, C.; Cai, S.; Lei, X.; Altoe, V.; Hong, F.; Urban, J. J.; Ciston, J.; Chan, E. M.; Liu, Y. Facile transformation of imine covalent organic frameworks into ultrastable crystalline porous aromatic frameworks. *Nat. Commun.* **2018**, *9*, 2998.

(12) Waller, P. J.; AlFaraj, Y. S.; Diercks, C. S.; Jarenwattananon, N. N.; Yaghi, O. M. Conversion of Imine to Oxazole and Thiazole Linkages in Covalent Organic Frameworks. *J. Am. Chem. Soc.* **2018**, *140*, 9099−9013.

(13) Jaradat, D. M. M. Thirteen decades of peptide synthesis: key developments in solid phase peptide synthesis and amide bond formation utilized in peptide ligation. *Amino Acids* **2018**, *50*, 39−68.

(14) Fracaroli, A. M.; Siman, P.; Nagib, D. A.; Suzuki, M.; Furukawa, H.; Toste, F. D.; Yaghi, O. M. Seven Post-synthetic Covalent Reactions in Tandem Leading to Enzyme-like Complexity within Metal-Organic Framework Crystals. *J. Am. Chem. Soc.* **2016**, *138*, 8352−8355.

(15) Wei, P.-F.; Qi, M.-Z.; Wang, Z.-P.; Ding, S.-Y.; Yu, W.; Liu, Q.; Wang, L.-K.; Wang, H.-Z.; An, W.-K.; Wang, W. Benzoxazole-Linked Ultrastable Covalent Organic Frameworks for Photocatalysis. *J. Am. Chem. Soc.* **2018**, *140*, 4623−4631.

(16) Stewart, D.; Antypov, D.; Dyer, M. S.; Pitcher, M. J.; Katsoulidis, A. P.; Chater, P. A.; Blanc, F.; Rosseinsky, M. J. Stable and ordered amide frameworks synthesised under reversible

conditions which facilitate error checking. *Nat. Commun.* **2017**, *8*, 1102.
(17) Bala, M.; Verma, P. K.; Sharma, D.; Kumar, N.; Singh, B. Highly efficient water-mediated approach to access benzazoles: metal catalyst and base-free synthesis of 2-substituted benzimidazoles, benzoxazoles, and benzothiazoles. *Mol. Diversity* **2015**, *19* (2), 263−272.
(18) Tang, J.; Wang, L.; Mao, D.; Wang, W.; Zhang, L.; Wu, S.; Xie, Y. Ytterbium pentafluorobenzoate as a novel fluorous Lewis acid catalyst in the synthesis of 2,4-disubstituted quinolines. *Tetrahedron* **2011**, *67*, 8465−8469.
(19) Thakur, M. S.; Nayal, O. S.; Sharma, A.; Rana, R.; Kumar, N.; Maurya, S. K. An Efficient Metal-Free Mono N-Alkylation of Anilines via Reductive Amination Using Hydrosilanes. *Eur. J. Org. Chem.* **2018**, *2018*, 6729−6732.
(20) Kandambeth, S.; Mallick, A.; Lukose, B.; Mane, M. V.; Heine, T.; Banerjee, R. Construction of Crystalline 2D Covalent Organic Frameworks with Remarkable Chemical (Acid/Base) Stability via a Combined Reversible and Irreversible Route. *J. Am. Chem. Soc.* **2012**, *134*, 19524−19527.
(21) Baxter, E. W.; Rietz, A. B. Reductive aminations of carbonyl compounds with borohydride and borane reducing agents. *Organic Reactions*; John Wiley and Sons, Inc.: Hoboken, NJ, United States, 2002; pp 1−714.
(22) Liu, Q.; Batt, D. G.; Delucca, G. V.; Shi, Q.; Tebben, A. J. Preparation of carbazole carboxamide compounds useful as kinase inhibitors. U. S. Patent 20100160303, June, 24, 2010.
(23) Pretsch, E.; Bühlmann, P.; Badertscher, M. IR Spectroscopy. *Structure Determination of Organic Compounds*, 4th ed.; Springer: Berlin, 2009; pp 269−335.
(24) Hu, X.-Y.; Zhang, W.-S.; Rominger, F.; Wacker, I.; Schröder, R. R.; Mastalerz, M. Transforming a chemically labile [2 + 3] imine cage into a robust carbamate cage. *Chem. Commun.* **2017**, *53*, 8616−8619.
(25) Johnson, R. L.; Schmidt-Rohr, K. Quantitative solid-state $^{13}C$ NMR with signal enhancement by multiple cross polarization. *J. Magn. Reson.* **2014**, *239*, 44−49.
(26) Duan, P.; Schmidt-Rohr, K. Composite-pulse and partially dipolar dephased multiCP for improved quantitative solid-state $^{13}C$ NMR. *J. Magn. Reson.* **2017**, *285*, 68−78.
(27) Szabo, M.; Agostino, M.; Malone, D. T.; Yuriev, E.; Capuano, B. The design, synthesis and biological evaluation of novel URB602 analogues as potential monoacylglycerol lipase inhibitors. *Bioorg. Med. Chem. Lett.* **2011**, *21*, 6782−6787.
(28) Hernández, A. S.; Hodges, J. C. Solid-Supported tert-Alkoxycarbonylation Reagents for Anchoring of Amines during Solid Phase Organic Synthesis. *J. Org. Chem.* **1997**, *62*, 3153−3157.
(29) Luca, O. R.; Wang, T.; Konezny, S. J.; Batista, V. S.; Crabtree, R. H. DDQ as an electrocatalyst for amine dehydrogenation, a model system for virtual hydrogen storage. *New J. Chem.* **2011**, *35*, 998−999.
(30) Rabbani, M. G.; Sekizkardes, A. K.; Kahveci, Z.; Reich, T. E.; Ding, R.; El-Kaderi, H. M. A 2D Mesoporous Imine-Linked Covalent Organic Framework for High Pressure Gas Storage Applications. *Chem. - Eur. J.* **2013**, *19*, 3324−3328.
(31) Alam, P.; Leung, N. L. C.; Cheng, Y.; Zhang, H.; Liu, J.; Wu, W.; Kwok, R. T. K.; Lam, J. W. Y.; Sung, H. H. Y.; Williams, I. D.; Tang, B. Z. Spontaneous and Fast Molecular Motion at Room Temperature in the Solid State. *Angew. Chem., Int. Ed.* **2019**, *58*, 4536.
(32) Liu, Y.; Ma, Y.; Zhao, Y.; Sun, X.; Gandara, F.; Furukawa, H.; Liu, Z.; Zhu, H.; Zhu, C.; Suenaga, K.; Oleynikov, P.; Alshammari, A. S.; Zhang, X.; Terasaki, O.; Yaghi, O. M. Weaving of Organic Threads into a Crystalline Covalent Organic Framework. *Science* **2016**, *351*, 365−369.